Tracking Channel Variations in a Time-varying Doubly-Spread Underwater Acoustic Channel

S. H. Huang
Dept. of Ocean Engineering
Ocean College
Zhejiang University
Hangzhou 310058, China
davidhuang@zju.edu.cn

T. C. Yang
College of Information Science &
Electronic Engineering
Zhejiang University
Hangzhou 310027, China
tcyang@zju.edu.cn

W. Xu
College of Information Science &
Electronic Engineering
Zhejiang University
Hangzhou 310027, China
wxu@zju.edu.cn

***Abstract*— Channel impulse responses (CIRs) are estimated for a doubly-spread acoustic channel in this paper by (1) estimating explicitly the path-dependent Doppler frequency shifts assuming a time-invariant CIR for individual blocks of data, and (2) estimating the time-varying CIR symbol by symbol including the phase change due to the Doppler. For the latter, a subspace based tracker is used to track the time variation of the channel basis vectors with their amplitudes tracked using a Kalman filter aided with a state-space model. For each method, the performance is measured by the normalized signal prediction error, the error between the data and the predicted signal based on the estimated CIRs, assuming the transmitted signal is known. Analysis of at sea data shows a 7 dB improvement in signal prediction error by tracking CIR using the model-based approach compared with the conventional methods based on explicit Doppler estimation.**

Keywords—Doubly spread acoustic channels; delay-Doppler-spread function; underwater acoustic communications; subspace tracking

I. INTRODUCTION

Underwater acoustic (UWA) channels are often referred to as doubly spread due to the extended multipath arrivals and path-dependent Doppler shifts/spreads. The low velocity of acoustic waves and the use of wideband modulation results in Doppler effect much more severe than those experienced in radio transmissions.

The linear time-varying channels can be described by the delay-Doppler spread function defined on the two-dimensional delay-Doppler plane [1]. For underwater acoustic communications, in order to remove the inter-symbol interferences, the equalizer must track the channel either by estimating/tracking the channel impulse responses or implicitly by adaptively adjusting the equalizer coefficients. For moving sources and/or receivers, one often removes the mean Doppler shift by resampling the data [2,3] (in the passband) based on the expected dilation /compression, and employs a phase-locked loop [4] to compensate residual mean Doppler shifts in the baseband. For time-varying channels, one assumes that the Doppler shift is time-invariant within a data block, and is estimated or adaptively adjusted on a block-by-block basis [5]. Note that for channels with large yet slowly varying Doppler, the assumption that the Doppler remains constant is far less restrictive than assuming that the channel impulse response is constant over an equivalent period of time [6].

Channel-estimation-based communications relies on the accurate estimation/tracking of the impulse response of the communication channels [6]. For broadband transmissions in shallow-water surface scattered acoustic channels, there are two major challenges: one is the excessive multipath delay spread that might extend over one hundred symbols. Another challenge is the severe Doppler shift and Doppler spread due to relative motion, stochastic surface fluctuation and medium inhomogeneity. For UWA channels, the Doppler to carrier frequency ratio is much higher than that of radio channels; therefore, a few Hz of Doppler can be very significant and thus need proper compensation. Furthermore, the global Doppler shift and Doppler spread on all propagation paths may be time-varying. Hence, it is much more difficult for a coherent receiver to combat such adverse conditions compared to the RF case.

For doubly spread UWA channels, direct tracking of channel variation symbol by symbol via adaptive filters is one approach. Alternatively, one may utilize the channel delay-Doppler-spread function representation to accommodate time variations of the channel impulse response within a data block of short duration. The dominant components of the delay-Doppler-spread function are then identified sequentially. Using those information, one may reconstruct the channel impulse responses and calculate the signal prediction error. Channel estimation and equalization approaches based on the delay-Doppler-spread function have previously been studied

978-0-933957-43-5 ©2015 MTS

[6-9]. The advantage of such approaches is its capability of tracking the first-order channel dynamics. In this paper, we investigate the use of direct channel tracking methods for underwater acoustic applications with mobile receiver and compare with that estimated from the delay-Doppler-spread function representation.

II. Doubly Spread Channel

The signal after propagating through a channel with an impulse response $h(t,\tau)$ is expressed at the receiver by

$$y(t) = \int h(t,\tau) s(t-\tau) d\tau + v(t) , \quad (1)$$

where t is referred to as geotime, τ is the delay time, $s(t)$ is the transmitted signal and $v(t)$ denotes the AWGN noise. For the purpose of discussions, one can express the channel impulse response by a series of multipath arrivals (rays) with different delay time τ_k

$$h(t,\tau) = \sum_{k=1}^{K} h_k(t) \delta(\tau - \tau_k(t)) , \quad (2)$$

where $h_k(t)$ is the amplitude of the kth multipath arrival, including the attenuation of the sound propagation. In the case of a moving source, for example, the ray arrival time is modified by the source motion,

$$\tau_k(t) = \tau_{k_0} + \frac{\mathrm{v} \cdot \cos\theta_k}{c} t \quad (3)$$

where v is the radial velocity of the source (v is positive for moving away), c is the sound speed in sea water, τ_{k_0} is the initial delay at the start of a block and θ_k is the grazing angle of the ray. Denoting $\beta_k = \frac{\mathrm{v} \cdot \cos\theta_k}{c}$ as the Doppler scaling factor and let $\alpha_k = 1 - \beta_k$, one finds

$$y(t) = \sum_{k=1}^{K} h_k(t)\, s\left(\alpha_k \cdot (t - \tau_{k_0}^{'})\right) + v(t) , \quad (4)$$

where $\tau_{k_0}^{'} = \tau_{k_0} / \alpha_k \simeq \tau_{k_0}$. One observes that individual multipath arrival signals have been compressed by a factor of α_k. This phenomenon is known as the Doppler effect. The signal is spread in time due to the different multipath arrivals and is spread in the Doppler when the multipaths have different grazing angles, i.e., if α_k has different values for different paths. It is noted that Doppler shift and spread can also be induced by the time variation of the channel. For example, in the presence of significant surface waves, even without relative motion between transmitter and receiver, different paths can have distinct and significant Doppler's (see e.g., Fig. 2 in [6]).

Channel estimation must take into account of the Doppler effect, including explicit or implicit estimation of the Doppler ratio α_k to minimize the channel estimation error. Expressing the transmitted signal in baseband,

$$\overline{s}(t) = \int_{-B/2}^{B/2} S(f_c + \tilde{f}) e^{j2\pi \tilde{f} t} d\tilde{f} ,$$

where S is the signal spectrum centered at the carrier frequency f_c, B is the signal bandwidth, and the baseband signal is denoted by the overhead bar, one find that the received signal is given in baseband by

$$\overline{y}(t) = \sum_{k=1}^{K} \overline{h}_k(t)\, \overline{s}\left(\alpha_k \cdot (t - \tau_{k_0})\right) e^{-j2\pi(\Delta f_k)t} + \overline{v}(t) , \quad (5)$$

where $\Delta f_k = \beta_k f_c$ is the Doppler shift of the kth multipath arrival. One observes that the source motion modifies the signal phase according to the Doppler shift as well as compresses/dilates the signal envelop (the baseband signal). For a narrow band signal, where $B << f_c$, one can approximate the source spectrum by its value at the carrier frequency, $S(f_c + \tilde{f}) \simeq S(f_c)\delta(\tilde{f})$. Therefore, we have

$$\overline{y}(t) \simeq \sum_{k=1}^{K} \overline{h}_k(t)\, \overline{s}(t - \tau_{k_0}) e^{-j2\pi(\Delta f_k)t} + \overline{v}(t) .$$

In this case, the received signal is the superposition of K time delayed, amplitude attenuated, and frequency shifted replica of $s(t)$.

For a broadband signal, the Doppler effect translates each frequency component by a different amount. One needs to correct for the signal compression/dilatation as for proper symbol synchronization. For this purpose, one first estimates the mean Doppler shift Δf, and determines the corresponding dominant Doppler scale factor $\alpha = 1 - \Delta f / f_c$. Resampling the signal in the passband to remove the mean Doppler, one obtains the following baseband signal

$$\begin{aligned} \overline{y}(t) &= \sum_{k=1}^{K} \overline{h}_k(t)\, \overline{s}\Big(\frac{\alpha_k}{\alpha}(t - \tau_{k_0})\Big) e^{-j2\pi\psi_k t} + \overline{v}(t/\alpha) \\ &\simeq \sum_{k=1}^{K} \overline{h}_k(t)\, \overline{s}(t - \tau_{k_0}) e^{-j2\pi\psi_k t} + \overline{v}(t/\alpha) \end{aligned} , \quad (6)$$

where we made the approximation $\frac{\alpha_k}{\alpha} \simeq 1$ and refer to $\psi_k = \Delta f_k - \Delta f$ as the residual Doppler shift, which may be time and path dependent. When the residual Doppler is left uncompensated, part of useful signals may be treated as additive noise, which could increase the overall noise variance considerably. One finds that the broadband signal, Eq (5), after proper resampling can be treated the same way as for a narrowband signal, Eq. (4).

Consider a digitized version of Eq. (6), sampled at one sample per symbol, namely, one sample per T_B, where T_B is the duration of a symbol, $T_B = 1/B$. Assuming that the channel impulse response $[h_1, h_2, \cdots, h_K]$ is time-invariant for a block of M symbols, one has

$$\begin{aligned} y_{n+m} &= s_{n+m} e^{-j2\pi\psi_1 m T_B} h_1 + s_{n+m-1} e^{-j2\pi\psi_2 m T_B} h_2 + \cdots \\ &\quad + s_{n+m-K+1} e^{-j2\pi\psi_K m T_B} h_K \end{aligned} , \quad (7)$$

where $0 \le m \le M-1$. In order to simplify the notation, time is set equal to zero at symbol n in Eq. (7).

A. Explicit Doppler Estimation

Equation (6) can be expressed in a matrix notation as follows

$$\begin{bmatrix} y_m \\ y_{m+1} \\ \vdots \\ y_{m+M-1} \end{bmatrix} = \begin{bmatrix} s_m & s_{m-1} & \cdots & s_{m-K+1} \\ s_{m+1}e^{j2\pi\psi_1 T_B} & s_m e^{j2\pi\psi_2 T_B} & \cdots & s_{m-K+2}e^{j2\pi\psi_K T_B} \\ \vdots & \vdots & \ddots & \vdots \\ s_{m+M-1}e^{j2\pi\psi_1 (M-1)T_B} & s_{n+M-2}e^{j2\pi\psi_2 (M-1)T_B)} & \cdots & s_{m+M-K}e^{j2\pi\psi_K (M-1)T_B} \end{bmatrix} \begin{bmatrix} h_1 \\ h_2 \\ \vdots \\ h_K \end{bmatrix} \tag{8}$$

which can be expressed in short as $\mathbf{y} = \mathbf{S}\mathbf{h}$. This delay-Doppler-spread based model accommodates the channel time variations just by explicitly populating the symbol sequence in Doppler domain [6-9].

There are two popular methods to estimate the Doppler frequency shift $[\psi_1, \psi_2, \cdots, \psi_K]$. The first uses a delay-Doppler ambiguity function, $\hat{\mathbf{y}}^H \mathbf{y} = \mathbf{h}^H \hat{\mathbf{S}}^H \mathbf{S}\mathbf{h}$, where $\hat{\mathbf{S}}$ is a bank of filters given by

$$\hat{\mathbf{S}} = \begin{bmatrix} s_m & s_{m-1} & \cdots & s_{m-K+1} \\ s_{m+1}e^{j2\pi\Delta f T_B} & s_m e^{j2\pi\Delta f T_B} & \cdots & s_{m-K+2}e^{j2\pi\Delta f T_B} \\ \vdots & \vdots & \ddots & \vdots \\ s_{m+M-1}e^{j2\pi\Delta f (M-1)T_B} & s_{m+M-2}e^{j2\pi\Delta f (M-1)T_B)} & \cdots & s_{m+M-K+1}e^{j2\pi\Delta f (M-1)T_B} \end{bmatrix}$$

where Δf denotes a bank of possible Doppler shift frequencies to be searched for. The Doppler shifts are estimated by those maximizing the ambiguity function or by the local maximum at each delay time (for each path arrival).

The other popular method uses the matching pursuit or orthogonal matching pursuit methods, which search for the kth path with a bank of filter

$$\hat{\mathbf{s}}_k = [s_{n-k+1}, s_{n-k}e^{j2\pi\Delta f T_B}, s_{n-k+1}e^{j2\pi\Delta f (2T_B)}, \ldots, s_{n-k+M+1}e^{j2\pi\Delta f (MT_B)}]^T,$$

which minimizes $|\mathbf{y} - \mathbf{s}_k^T h_k|^2$. The kth path contribution is subtracted for $\mathbf{y}$ and the process repeats itself until it reaches a minimum predetermined value.

B. Symbol Based Channel Estimation – Implicit Doppler Estimation

We propose a new method to estimate the channel impulse response, assuming a time varying channel impulse response. As opposed to the block constant assumption in (7), the index system of a time-varying case can be revised as

$$y(n) = s(n)h^*(n,1) + s(n-1)h^*(n,2) + \cdots + s(n-K+1)h^*(n,K), \tag{9}$$

where

$$\begin{aligned} h(n,1) &= h_1^* e^{j2\pi\psi_1 nT_g} \\ h(n,2) &= h_2^* e^{j2\pi\psi_2 nT_g} \\ &\vdots \\ h(n,K) &= h_K^* e^{j2\pi\psi_K nT_g} \end{aligned}.$$

The discrete-time sampled CIRs is represented by $h(n,k) \equiv h(t_n = nT_g, \tau_k = kT_B)$, where T_g is the time separation between CIRs and T_B was defined previously. Therefore, estimating the Doppler shift is included in the estimation of a time-varying channel impulse response, including particularly its phase. We will estimate the time-varying channel impulse response via the signal subspace, with a model based approach where the channel coefficient is tracked using a Kalman filter as described below in Sec. III.

III. Adaptive Subspace-Tracking With Reduced-Rank Model-Based Estimation (ASRMAE)

The purpose of the ASRMAE method is to track the channel variation in the signal subspace and at a fast rate – symbol by symbol instead of block by block. Let $\mathbf{h}(n) = [h(n,1), h(n,2), \cdots, h(n,K)]^T$ denotes the vector of the CIR taps at time nT_g. Here the channel dimension K is large enough to cover multipath delay spread. The discrete-time input-output relation (9) can be denoted as

$$y(n) = \mathbf{h}^H(n)\mathbf{s}(n) + v(n) \tag{10}$$

where $\mathbf{s}(n)$ is the transmitted data vector and $v(n)$ is the AWGN noise sample. For the purpose of discussion, the received signal is assumed to be sampled at the transmitted symbol rate. For experimental data processing, the data are fractionally sampled at a rate $\rho = 2$ samples per symbol. The CIR can be expressed in terms of the eigenvectors

$$\begin{aligned} \mathbf{h}(n) &= z_1(n)\mathbf{q}_1(n) + z_2(n)\mathbf{q}_2(n) + \cdots + z_K(n)\mathbf{q}_K(n) \\ &= \mathbf{Q}(n)\mathbf{z}(n) \end{aligned}, \tag{11}$$

where $\mathbf{Q}(n) = [\mathbf{q}_1(n), \mathbf{q}_2(n), \cdots, \mathbf{q}_K(n)]$ is the eigenvector matrix of

$$\mathbf{R}_{\mathbf{h}}(n) = E\{\mathbf{h}(n)\mathbf{h}^H(n)\} = \mathbf{Q}(n)\mathbf{\Lambda}(n)\mathbf{Q}^H(n),$$

and $\mathbf{\Lambda}(n) = diag([\chi_1(n), \chi_2(n), \cdots \chi_K(n),])$ is a diagonal matrix of the corresponding eigenvalues, in descending order. The vector $\mathbf{z}(n) = [z_1(n), z_2(n), \cdots, z_K(n)]^T$ is referred to as the channel component vector. The hyperspace occupied by the eigenvectors associated with the r largest eigenvalues are referred as the signal subspace, and the rest eigenvector space are referred to as noise subspace. Note that the reason for channel decomposition (11) is to separate the signal from the noise. One finds that the signal has a small dimension $r\,(r \ll N)$ and the r leading channel components and signal basis may be used to reconstruct the CIR as

$$\hat{\mathbf{h}}_r(n) = \hat{z}_1(n)\mathbf{q}_1(n) + \hat{z}_2(n)\mathbf{q}_2(n) + \cdots + \hat{z}_r(n)\mathbf{q}_r(n) \\ = \mathbf{Q}_r(n)\hat{\mathbf{z}}_r(n) \quad (12)$$

The reduced rank approximation (12) results in a significant reduction of the computational complexity, allowing the channel tracking algorithms to focus on tracking only the signal components and basis vector. One observes experimentally that the basis vectors often vary much more slowly than the channel components $\mathbf{z}(n)$ and the signal subspace dimension r is small compared to channel dimension K [10,11].

A. Signal Subspace Tracking

For slowly time-varying channels, the signal subspace basis matrix $\mathbf{Q}_r$ can be treated as a constant and be estimated by eigenvector decomposition (EVD) of the channel covariance matrix. However batch EVD is unsuitable for sequential adaptive processing because it involves very heavy computations. To overcome this difficulty, a number of adaptive algorithms for sequential adaptive eigenvector decomposition have been proposed in the literature. For the application discussed in this paper, a choice that has been shown to be a good tradeoff between complexity and performance is the PASTd algorithm proposed in [12]. One consider the following cost function

$$J(\mathbf{W}) = \mathbf{E}\,\|\,\mathbf{h}(n) - \mathbf{W}\mathbf{W}^H\mathbf{h}(n)\,\|^2 \\ = \mathrm{tr}(\mathbf{R_h}) - 2\mathrm{tr}(\mathbf{W}^H\mathbf{R_h}\mathbf{W}) + \mathrm{tr}(\mathbf{W}^H\mathbf{R_h}\mathbf{W}\cdot\mathbf{W}^H\mathbf{W}), \quad (13)$$

where $\mathbf{W} \in C^{K\times r}$ is a matrix of dimension K x r. It has been proved [12] that $\mathbf{W}$ is a stationary point of $J(\mathbf{W})$ iff $\mathbf{W} = \mathbf{Q}_r\mathbf{U}$, where $\mathbf{Q}_r \in C^{K\times r}$ contains any r distinct eigenvectors of $\mathbf{R_h}$ and $\mathbf{U} \in C^{r\times r}$ is an arbitrary unitary matrix. At each stationary point, $J(\mathbf{W})$ has a value equaling the sum of the noise space eigenvalues, $\sum_{k=r+1}^{K} \chi_k$, associated with the noise eigenvectors. Moreover, $J(\mathbf{W})$ attains a global minimum at which the column space of $\mathbf{W}$ equals to the subspace spanned by the r dominant eigenvectors of $\mathbf{R_h}$, that is, the signal subspace of $\mathbf{R_h}$ (see Theorems 1,2 in [12]). Therefore a global convergence of solving $J(\mathbf{W})$ is guaranteed by tracking the signal subspace of $\mathbf{R_h}$. The purpose of the PASTd algorithm is to track the dominant r eigenvectors $\mathbf{W}(n) = \mathbf{Q}_r(n)$ as a function of time (symbol by symbol). It is assumed that the dominant eigenvectors can be estimated reliably from a coarse estimate of CIR, such as that obtained using the LMS method $\hat{\mathbf{h}}^{LMS}(n)$. The underlying reason is that the error between $\hat{\mathbf{h}}^{LMS}(n)$ and the true $\mathbf{h}(n)$ is caused by the small eigenvalues and the associated eigenvectors, which are difficult to estimate and track accurately. Since one is interested only in the signal subspace occupied by the large eigenvalues and their eigenvectors, $\hat{\mathbf{h}}^{LMS}(n)$ will be sufficient for our purposes.

B. Model-based tracking of channel components

For the model-based approach, one assumes that the channel component $\mathbf{z}_r(n)$ follows a p-order Markov process for the discrete-time random process

$$\mathbf{z}_r(n) = \sum_{l=1}^{p} \mathbf{\Phi}(l)\mathbf{z}_r(n-l) + \boldsymbol{\eta}(n), \quad (14)$$

where $\mathbf{z}_r(n) = [z_1(n), z_2(n), \cdots, z_r(n)]^T$ is the channel component vector defined previously, $\mathbf{\Phi}(l) \in \mathbb{C}^{r\times r}$ represents the state transition matrix, $\boldsymbol{\eta}(n) \in \mathbb{C}^r$ is the process noise vector. With this assumption, one can estimate the state transition matrix $\mathbf{\Phi}(l)$ and the process noise covariance $\mathbf{R}_{\boldsymbol{\eta}} = E\{\boldsymbol{\eta}(n)\boldsymbol{\eta}^H(n)\}$ from the covariance matrix of the channel components $\mathbf{R_z} = E\{\mathbf{z}_r(n)\mathbf{z}_r^H(n)\}$ with $E[z_i(n)z_j^*(l)] = R_i(n-l)\delta_{ij}$ as described in [10], where $\hat{\mathbf{z}}_r(n) = \mathbf{Q}_r^H(n)\hat{\mathbf{h}}^{LMS}(n)$ is obtained by projecting the $\hat{\mathbf{h}}^{LMS}(n)$ onto the signal subspace and $\eta_i(n)$ and $z_i(n-m)$ are independent random variables, namely, $E[\eta_i(n)\cdot z_i^H(n-m)] = 0$ for $m \neq 0$. Solving for all these parameters involves only scalar computations due to decoupling; hence both the complexity and risk of over-parameterization are low. Channel tracking will be conducted using a Kalman filter by (recursively) minimizing the signal prediction error. Expanding CIR in terms of the leading eigenvectors, $\hat{\mathbf{h}}_r(n) = \mathbf{Q}_r(n)\mathbf{z}_r(n)$, one finds

$$\mathrm{y}(n) = \mathbf{d_z}^T(n)\mathbf{z}_r(n) + v(n), \quad (15)$$

where $\mathbf{d_z}^T(n) = \mathbf{s}^T(n)\mathbf{Q}_r(n)$ is the transmitted data vector projected on the (time varying) signal subspace. Equations (14) and (15) can be expressed in a compact state-space form (model)

$$\mathbf{Z}(n) = \mathbf{\Phi_Z}\mathbf{Z}(n-1) + \mathbf{N}(n) \\ \mathrm{y}(n) = \mathbf{D}(n)\mathbf{Z}(n) + v(n), \quad (16)$$

where $\mathbf{D}(n) = [\mathbf{d_z}^T(n)\ \mathbf{0}_{1\times r(p-1)}]$ and
$\mathbf{Z}(n) \triangleq [\mathbf{z}_r{}^T(n), \cdots, \mathbf{z}_r{}^T(n-p+1)]^T$,
$\mathbf{N}(n) = [\eta^T(n)\ \mathbf{0}_{1\times r(p-1)}]^T$,
and the state transition matrix $\mathbf{\Phi_Z}$ is given by

$$\mathbf{\Phi_Z} = \begin{bmatrix} \mathbf{\Phi}(1) & \mathbf{\Phi}(2) & \cdots & \mathbf{\Phi}(p) \\ \mathbf{I}_K & \mathbf{0}_K & \cdots & \mathbf{0}_K \\ \vdots & \ddots & \ddots & \vdots \\ \mathbf{0}_K & \cdots & \mathbf{I}_K & \mathbf{0}_K \end{bmatrix} \quad (17)$$

The Kalman filter algorithm works as follows (for details see [10]). Given the estimated current state vector $\mathbf{Z}(n)$, one calculates the (*a priori*) signal prediction error $\xi(n) = y(n) - \mathbf{D}(n)\mathbf{Z}(n)$, known as the innovation. Based on $\mathbf{Z}(n)$ and the innovation, one estimates the next state vector $\mathbf{Z}(n+1)$ as follows: $\mathbf{Z}(n+1) = \mathbf{\Phi_Z}\mathbf{Z}(n) + \mathbf{G}(n)\xi(n)$, where

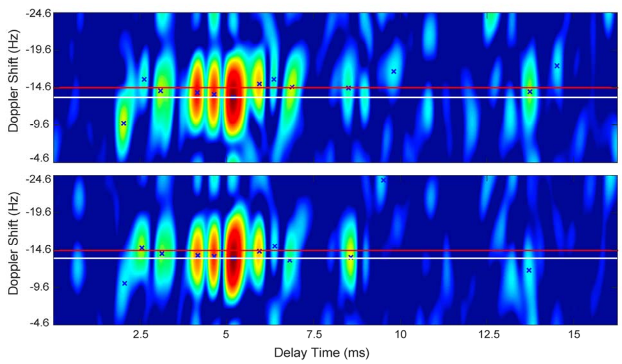

Fig. 1. Delay-Doppler-spread function of two consecutive m-sequence blocks (block 72, 73). The red line denotes a coarse estimated mean Doppler. The residual Doppler (marked by white solid line) are 1.3 and 1.05 Hz for block 72 and 73, respectively. The cross mark indicate the Doppler shift of individual arrival.

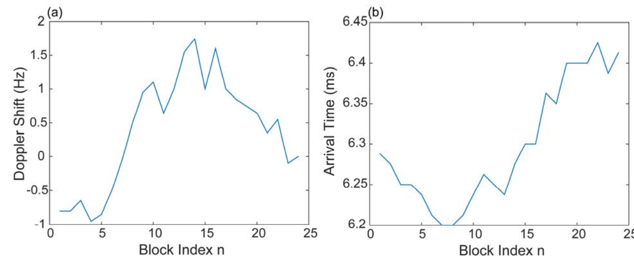

Fig. 2. (a) Residual mean DOPPLER of main arrival (frequency difference between white and red solid line in Fig. 1) of the first 24 blocks. In this data, the Residual mean Doppler swing (approximately) between +/- 1.5 Hz. (b) Arrival time fluctuation of the main arrival in the first 24 blocks. In this data set, the arrival time difference is more than 0.2 ms, which is approximately one symbol duration.

$\mathbf{\Phi_Z Z}(n)$ is the prediction based on the state-space model (16), and $\mathbf{G}(n)\xi(n)$ is the update (or correction) to the prediction, where matrix $\mathbf{G}(n)$ is known as the Kalman gain. The above process repeats itself, each time incrementing n by 1, a new signal subspace $\mathbf{Q}_r(n)$ is estimated followed by a new estimated state vector. At each step, the Kalman filter attempts to balance the prediction with the correction to produce a statistically optimal estimate of the underlying system state. The algorithm outputs the predicted CIR $\hat{\mathbf{h}}_r^{ASRMAE}(n) = \hat{\mathbf{Q}}_r(n)\mathbf{z}_r(n)$, and the signal prediction error $\xi(n)$. The latter is used in Sec. IV to evaluate the algorithm performance.

IV. ACOUSTIC COMMUNICATION DATA

To demonstrate the performance of various channel estimation/tracking algorithms, data collected at sea has been analyzed and the results are presented in this section. One may explicitly estimate the delay-Doppler spread function and convert the information to channel impulse response or by an implicit approach where channel taps are tracked directly using either LMS or ASRMAE algorithms proposed in Sec. III. In all the cases, the receivers are operated in the training mode where the transmitted symbols are assumed perfectly known. The experiment was set up using a fixed receiver and a moving sound source towed by a ship [13]. This sound source projects continuous m-sequence signals modulated to 17 kHz carrier frequency with a bandwidth of 4 kHz. The sound speed profile is near a constant except toward the surface and bottom and the water depth is around 70m. After a coarse resample is performed at passband to remove mean dominant Doppler, the received signal is brought to baseband and sampled at a rate of 2 samples per symbol. There was no error correction code used on the transmitter sequences during the experiment.

A. Channel Characteristics of Doubly-Spread Channel

Linear time-varying channels can be described by the delay-Doppler spread functions defined on the two-dimensional delay-Doppler plane. In this section, the received data are processed to estimate the delay-Doppler spread function by using matched filtering, which includes computing the cross-ambiguity function (CAF) of the transmitted and received signals. Physical arguments and experimental evidence indicate that acoustic channels tend to be sparse in both time and frequency domain, i.e., the delay-Doppler spread function has few nonzero elements compared with its dimension. It is expected that the channel estimation performance will be improved if the sparse structure of the channel is taken into account [6-9].

The result of delay-Doppler-spread function from two consecutive m-sequence blocks (72 and 73) is displayed in Fig. 1, from where one notice the arrival gain, path Doppler and arrival time are all more or less changing. This figure shows the mean Doppler shift is approximately 14.6 Hz (mean of 200 m-sequence blocks) and is marked by a red solid line. One defines the frequency deviation of each block, calculated from center frequency of the main arrival (marked by white solid line) to mean Doppler shift (marked by red solid line), as residual mean Doppler shift. The residual mean Doppler shift for block 72 and 73 are 1.3 and 1.05 Hz, respectively.

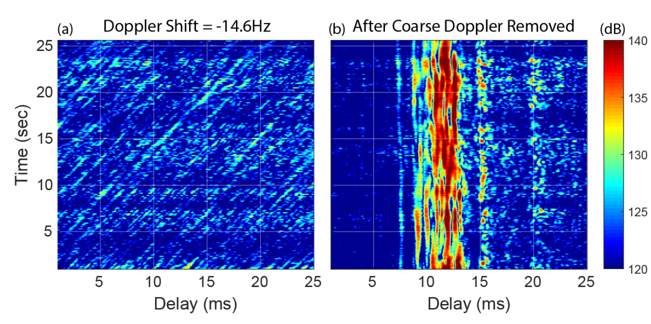

Fig. 3. Rough channel estimation results. Fig. 2(a) shows the rough CIR estimate without resample of the received signal. The slope of the scratch pattern in (a) can be used as a rough Doppler shift estimate. For this case with $f_c = 17k$ Hz, the mean Doppler scaling factor $\alpha = -0.000858$, which corresponds to mean Doppler shift of -14.6 Hz. After resample of the received signal at passband, the roughly estimated CIR is shown in (b).

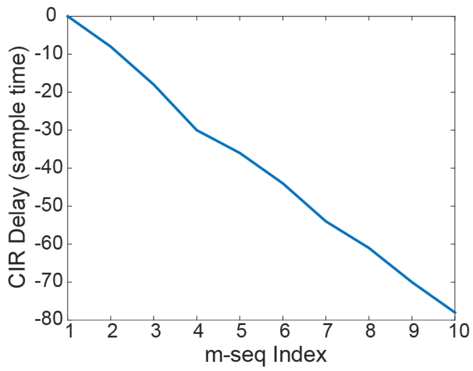

Fig. 4. Coarse DOPPLER shift estimation using slope of scratch pattern displayed in Fig. 3(a)

In Fig. 1, we use a cross mark to indicate the frequency shift of each arrival. One notice that each arrival has slightly different Doppler shift and may change between blocks. The frequency deviation of individual path relative to residual mean Doppler (white solid line) is termed path residual Doppler. The mean residual Doppler shift and (main) path arrival delay change with time and are displayed in Fig. 2.

If one estimate CIR using received signal directly without signal rescaling, the result is a scratch pattern as shown in Fig. 3(a). The slope of this pattern can be modeled by (3) and is primarily due to relative motion. One may estimate the Doppler scaling factor based on the slope estimate of such pattern (shown in Fig. 4) or use the method proposed in [2,3]. Note that this scaling factor is only a roughly estimated value; the time-varying nature of the Doppler, estimation error and resampling inaccuracy go into residual Doppler ψ_k . Further estimation/tracking mechanism is needed to compensate the residual path Doppler. With the knowledge of Doppler scaling factor α , one can resample the received signal to approximately remove the mean Doppler shift. The resulted CIR estimation is shown in Fig. 3(b). The residual mean Doppler is a function of time and may vary slightly block by block as shown in Fig. 2(a), where the value swings approximately between +/- 2 Hz. The arrival delay is also slowly varying with time as shown in Fig. 2(b) where arrival time (of main arrival) fluctuates more than 0.2 ms back and forth (approximately one symbol duration).

B. CIR Estimation/Tracking Performance

Fig. 5 plots the normalized signal prediction error for the various algorithms given below. The received signals are first resampled using the estimated Doppler scale factor ($\alpha \approx 1.00086$, indicates the sound source are moving away). LMS algorithm is first applied to track channel variations, including residual Doppler shift reflected on the fluctuating CIR taps. This is the first method. The normalized mean signal prediction error in the first 100 blocks (12.775 Sec.) is -7.04 dB as shown in Fig. 5(a) by the green solid line. The second method reconstruct the CIR from delay-Doppler function estimation assuming all 100 blocks have a common mean

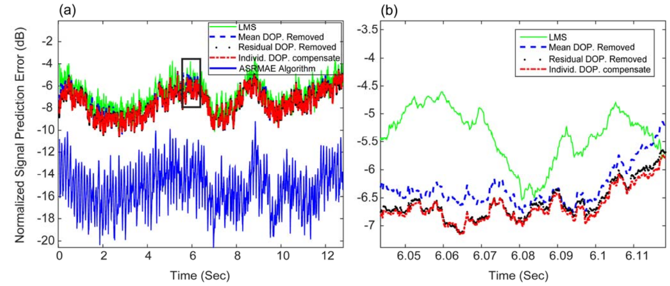

Fig. 5. (a) Comparison of mean signal prediction error for various approaches. For LMS algorithm, MSE = -7.04 dB while it is -14.2 dB for ASRMAE algorithm. (b) Zoom in of the rectangle black box in (a)

Doppler shift. The third method estimates the CIR block by block including the residual mean Doppler shift, assuming all paths have the same Doppler shift, which is the most common assumption. The fourth method estimates the CIR block by block including the path residual Doppler shift, assuming paths have different Doppler shift as when the receiver is not far away from the source [7-9]. For the above methods (methods 2~4), the CIR is estimated using the CAF at the corresponding Doppler frequencies. The result is shown in Fig. 5(a) and the local zoom in at time around 6.04~6.12 seconds (marked by a black rectangle box) is shown in Fig. 5(b). Based on Fig. 5(b), one notes that the channel tracking performance is improved by considering the path dependent Doppler shift. For the present case, the improvement may not be significant enough, compared with the increased computational complexity. This may not be the case when the paths exhibit significantly different Doppler shifts [7-9]. Figure 5(a) also displays the tracking performance achieved by using ASRMAE algorithms (blue solid line). The tracking performance using ASRMAE algorithm can be improved by approximately 7 dB, compared with the above methods.

C. Doppler Tolerance

A major design consideration is the degree of accuracy required from the coarse Doppler estimation and resampling, which is entirely dependent on the amount of residual Doppler that can be tolerated by the receiver/demodulator system. Stated differently, if the coarse estimate of the mean Doppler is in error, the residual Doppler will also be large and needs to more accurately estimated, which will test the limitation of the various residual Doppler shift and compensation methods (such as that using the phase locked loop). One finds that the proposed ASRMAE algorithm not only has the lowest tracking error but also can tolerate larger residual Doppler shifts. Fig. 6 shows while residual Doppler shift increase (from 0 ~ -4 Hz or 0 ~ 5 Hz), the ASRMAE algorithm has less than 2dB performance degradation. This suggests a higher tolerance to the error in coarse Doppler estimation and data re-sampling. Doppler estimation error of 3×10^{-4} would be good enough for ASRMAE algorithm to perform reasonably well. In the meantime, LMS algorithm is less capable of tracking channel with residual Doppler. With the same amount of residual Doppler shift, LMS algorithm has approximately 4 dB performance degradation.

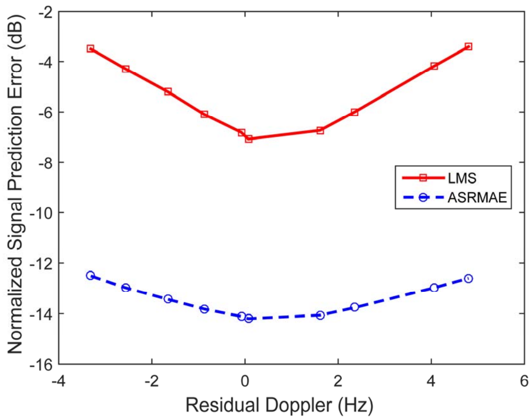

Fig. 6. Algorithm sensitivity to residual Doppler. In zero residual Doppler, ASRMAE outperforms LMS algorithm by 7 dB. As residual Doppler increase, normalized signal prediction error of both algorithms increase. However, the ASRMAE is far less sensitive to residual Doppler (slope of ASRMAE is approximately half of that of LMS). This indicates ASRMAE has better capability to track Doppler shift than the LMS algorithm.

V. SUMMARY

This paper study a number of methods for Doppler estimations and evaluate their performance in terms of the normalized signal prediction error. It is shown that the ASRAME method achieves a ~7 dB improvement in channel estimation than the conventional methods that estimate the Doppler shifts explicitly assuming a block invariant CIR.

REFERENCES

[1] P. A. Bello, “Characterization of randomly time-variant linear channels,” *IEEE Trans. Comm. Syst.* , vol. 11, no. 4, pp. 360 - 393, Dec. 1963.

[2] B. S. Sharif, J. Neasham, O. R. Hinton, and A. E. Adams, “A computationally efficient Doppler compensation system for underwater acoustic communications,” *IEEE J. Ocean. Eng.,* vol. 25, no. 1, pp. 52-61, Jan. 2000.

[3]. T. C. Yang, “Underwater telemetry method using Doppler compensation,” U.S. Patent No. 6,512,720 (Jan. 2003).

[4] M. Johnson, L. Freitag, and M. Stojanovic, “Improved Doppler tracking and correction for underwater acoustic communications,” *Proc. ICASSP '97,* vol. 1, pp. 575-578, Apr. 1997.

[5] B. Li, S. Zhou, M. Stojanovic, L. Freitag, and P. Willett, “Multicarrier communication over underwater acoustic channels with nonuniform Doppler shifts,” *IEEE J. Ocean. Eng.,* vol. 33, no. 2, pp. 198-209, Apr. 2008.

[6] W. Li and J. C. Preisig, “Estimation of rapidly time-varying sparse channels,” *IEEE J. Ocean. Eng.,* vol. 32, no. 4, pp. 927-939, Oct., 2007.

[7] X. Jiang, W.-J. Zeng, and X.-L. Li, “Time delay and Doppler estimation for wideband acoustic signals in multipath environments,” *J. Acoust. Soc.Am*. 130, pp. 850–857, 2011.

[8] W.-J. Zeng, and W. Xu, “Fast estimation of sparse doubly spread acoustic channels,” *J. Acoust. Soc. Am*. 131, pp. 303-317, 2012.

[9] F. Qu, X. Nie, and W. Xu, “A two-stage approach for the estimation of doubly spread acoustic channels,” *IEEE J. Ocean. Eng.,* vol. 40, no. 1, pp. 131-143, 2015

[10] S. H. Huang, J. Tsao, T. C. Yang, and S.-W. Cheng, “Model-based signal subspace channel tracking for correlated underwater acoustic communication channels,” *IEEE J. Ocean. Eng.,* vol. 39, no. 2, pp. 343-356, Apr. 2014.

[11] S. H. Huang, T. C. Yang, and J. Tsao, “Improving channel estimation for rapidly time-varying correlated underwater acoustic channels by tracking the signal subspace,” *Ad Hoc Netw.*, 2014, http://dx.doi.org/10.1016/j.adhoc.2014.09.014.

[12] B. Yang, “Projection approximation subspace tracking,” *IEEE Trans. Signal Processing,* vol. 43, no. 1, pp. 95 - 107, Jan. 1995.

[13] T. C. Yang, and W.-B. Yang, “Low probability of detection underwater acoustic communications using direct-sequence spread spectrum,” *J. Acoust. Soc. Am*., 124, pp. 3632-3647, 2008.